Advanced Elastomeric Materials

Chapter 5: Conductive Elastomers and Their Electronic Applications

5.1. Introduction

There had been an extensive variety of exertions to develop conductive elastomers that fulfill both electrical conductivity and mechanical stretchability, as a response to increasing demands on wearable devices. This chapter analyzes the significant development in conductive elastomers completed in 3 application fields of stretchable technology: stretchable sensors, stretchable energy harvesters, and stretchable electronics. Different combinations of non-stretchable conductive materials and insulating elastomers had been studied to understand optimal conductive elastomers (Kim and Rogers, 2008; Ahn and Je, 2012). It is noted that similar structures and similar material combinations had frequently been employed in diverse fields of application. In terms of cyclic operation, stretchability, and overall performance, fields like as stretchable pressure/strain sensors and stretchable conductors had attained great advancement, while other fields like stretchable thermoelectric energy harvesting and stretchable memories are in their beginning. It is worth stating that there are still problems to overwhelmed for the further development of stretchable technology in the relevant fields, which comprise the device structure and simplification of material combination, reliability, and securement of reproducibility, and the formation of easy fabrication methods. By this review article, both the obstacles and progress related with the relevant stretchable technologies would be understood more obviously (Someya et al., 2005; Rogers et al., 2010).

The demand for stretchable devices had been ever-rising as novel technology fields like intelligent robotics, body conformable devices, stretchable electronics, and wearable devices, had emerged (Kim and Rogers, 2008). For example, keen sensory skins are needed to execute advanced robots that could interact well with humans and appropriately respond to the environment without exterior control (Chou et al., 2015). Keeping pace with this increasing need for novel technology, a movement of searching for novel materials that could afford good mechanical elasticity and also high electrical conductivity had surged (Faez et al., 2002). Though a diversity of conducting polymers, like polypyrrole (PPY), polyaniline (PANI), polyacetylene (PA), and poly(3,4-ethylene dioxythiophene (PEDOT) had been developed for various applications, their extensive usage is limited through their poor mechanical properties. For instance, a (PEDOT: PSS) poly(3,4-ethylene dioxythiophene): poly(styrene sulfonic acid) film, which is extensively employed in organics founded optoelectronic devices and plastic electronics, displays high electrical conductivity up to 1000 S/cm; however, its breaking strain is under 10% (Lang et al., 2009). This level of forbearance to strain is not suitable for the above-stated applications.

On the contrary, elastomers like SBR (styrene-butadiene rubber), polyurethane (PU), poly(dimethylsiloxane (PDMS), natural rubber (NR), and ethylene-propylene-diene monomer (EPDM) are characterized by poor conductivity, high, reversible deformation (>200%) (Kim et al., 2011). Traditionally, they had been utilized mainly for structural, industrial, and household products,

and numerous fillers had been integrated into them to fortify mechanical properties like Young's modulus and tensile strength (Liu et al., 2015). Excitingly, certain conductive fillers characterized by a family of carbon matters, like graphites, carbon blacks (CBs), and carbon nanotubes (CNTs) had been introduced to transmute the resin from an insulator to a conductor. Though this approach needs a substantial amount of filler to be added, occurring an extreme loss of the material's elasticity; however, the degradation of elasticity could be reduced for CNT-elastomer mixtures, where conductive CNT categorization networks could be formed through the addition of just a little amount of CNTs (Benight et al., 2013; Chortos and Bao, 2014).

For the sake of the instantaneous gratification of good elasticity and high electrical conductivity, certain groups had attempted to alter the molecular structures of elastomers. Doping SBR with antimony pentachloride ($SbCl_5$) and iodine (I_2), and producing graft copolymers composed of PANI and PU are typical instances (Abbati et al., 2003). Though, these methods need elaborate modification of experimental conditions and are still to endorse their long-term reliability. A more practical and easy method of tackling the goal is to create a blend comprising of an elastomer and a conducting polymer (Hansen et al., 2007). In this structure, the conducting polymer shows a role in enhancing the conductivity of the mixture; however, the elastomer condenses the material stretchable. When 11.5% of PANI by volume portion was added to PU, the material's conductivity enhanced by six orders of magnitude, however, keeping a high stretchability of 200%. For a PEDOT-PU merger, a high conductivity of 100 S/cm was revealed, even under an elongation of >100%. Usually, the electrical conductivity of a blend rises at the cost of mechanical properties as the portion of the conductive part enhances. Therefore, elaborate material design is essential to accomplish detailed specifications needed for precise applications (Wang et al., 2001; Bhadra et al., 2009).

In this review, various exertions to realize conductive elastomers and the latest progress are debated. Owing to the vastness of earlier works, some representative outcomes in the fields of sensors, electronics, and energy harvesting would be introduced. Notably, similar material combinations and similar strategies had sometimes been accepted in diverse fields of application. Although this review, not only accomplishments made till yet, however tasks to be solved would also be deliberated (Tamai, 1982; Chou et al., 2015).

5.2. Stretchable Electronics

The scope of stretchable electronics is very extensive, comprising memories, stretchable logic gates, and stretchable display units. Although the relevant devices had diverse structures, they are usually organized with basic elements, like transistors, interconnects, dielectrics, and light-emitting diodes (LEDs). One of the significant strategies for executing stretchable electronics is a mixture of active, rigid components, and stretchable interconnects, which accommodate exterior strains (Lacour et al., 2004; Sun et al., 2006). Although to realize actual stretchable electronics, entire components are required to be stretchable. From the part of materials, this needs semiconductors, conductors, and

dielectrics, all of them are stretchable. In this portion, stretchable conductors and certain representative stretchable devices are concisely reviewed (Faez et al., 2002; Saleem et al., 2010).

5.2.1. Stretchable Conductors

Two kinds of metal structures (*for example.*, serpentine structures and wavy structures) had been extensively explored as stretchable conductors. Wavy metal structures are made from metal films placed on the pre-patterned or strained elastomeric substrate (Kim et al., 2008), and their alterable stretchability is comparatively low (<20%). On the other side, serpentine metal structures are 2D or 3D ranges of a reiterating horseshoe-shaped unit. Hsu *et al.* confirmed the ultimate elongation of 250% and the reliability of 40,000 cycles at a 30% elongation, utilizing polyimide enhanced Cu serpentine structures (Hsu et al., 2011; Hilbich et al., 2015). Though these techniques proved their efficiency, they usually need a multi-step procedure comprising a costly lithography step (Das and Prusty, 2012; Balint et al., 2014).

Another method is to employ elastomeric compounds. The elastomeric compounds might be elastomer conducting polymer mixtures, elastomeric compounds incorporating metal nanostructures or carbon nanostructures, and polymer blends integrating nanostructures of the conductive materials (Faez et al., 1999; Stoyanov et al., 2013). Nearly two decades before, Fu et al. (1998) made elastomeric PU—PPY compound foams through *in situ* polymerization of pyrrole in pre-formed PU foams, and conductivity of 10^{-5} S/cm and elongation at the halt of 160% was attained from a 6 wt.% PPY comprising composite (Lee and Khang, 2012; Chen et al., 2013). The less conductivity of the compound, which was one of the major problems with techniques utilizing PU foams, had been improved through introducing conductive nanostructures. For instance, Ge *et al.* made-up Ag nanowire PU sponge PDMS stretchable conductors through a simple solution-dipping technique, and definite high conductivity of 19.2 S/cm, and a resistance change $(\Delta R/R_0)$ of 160% at a 100% strain (Ge et al., 2013). Rather than PU foams, Park et al. (2012) created 3D PDMS structures utilizing proximity field nanopatterning, and formed transparent, stretchable conductors through infiltrating liquid metal, EGaIn (eutectic gallium-indium), into the 3D PDMS (Figure 5.1(a)–(c)). The 3D PDMS-EGaIn stretchable conductors presented tremendously high conductivity (24,100 S/cm), even below strains of >200%, and good stretching cycle achievement (Figure 5.1(d) and (e)) (El-Tantawy et al., 2009; Khan et al., 2010).

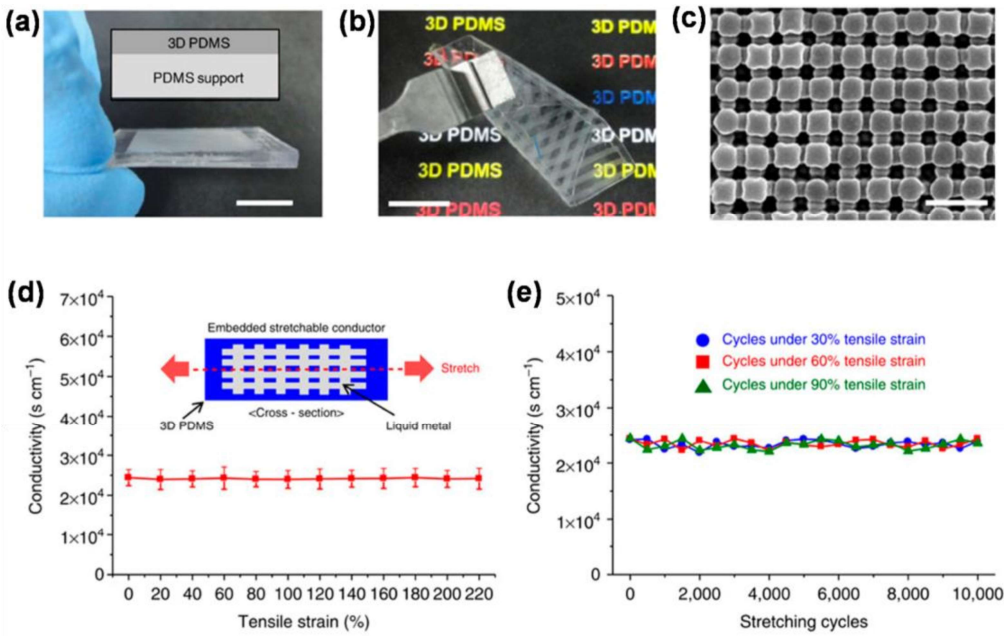

Figure 5.1. *Optical images of (a) a 3D PDMS (poly(dimethylsiloxane) film on PDMS support; and (b) a folded 3D PDMS film. Scale bar, 1 cm; (c) top view SEM image of net made 3D PDMS film. Scale bar, 1 μm; (d) conductivity of 3D PDMS-EGaIn (eutectic gallium-indium) stretchable conductor below strains of up to 220%; (e) conductivity variation relying on the number of stretching-releasing cycles under diverse strains.*

Source: https://www.scholars.northwestern.edu/en/publications/three-dimensional-nanonetworks-for-giant-stretchability-in-dielec.

Hansen et al. (2007) made PU-PEDOT combinations from liquid mixtures of EDOT and fluctuating amounts of PU liquefied in tetrahydrofuran (THF) without involving porous elastomers (Rogers and Huang, 2009). They stated a good conductivity of 10–50 S/cm at a 200% strain for the mixtures. As a similar approach, Noh (2014) made PDMS-PEDOT: PSS combinations through introducing a miscibility increasing copolymer, poly(dimethylsiloxane-*b*-ethylene oxide (PDMS-*b*-PEO), and revealed a conductivity up to 2 S/cm and a fracture strain of 75% (Noh, 2014). Single-walled CNTs (SWCNTs) and multi-walled CNTs (MWCNTs) had been very extensively employed to transmute insulating elastomers to conductors. Kim et al. (2014) made SWCNT-PDMS composites through backfilling SWCNT aerogels and noticed conductivities of 70–108 S/m and a little resistance alteration of 14% at a tensile strain of 100%. Shin et al. (2010) used the same approach, in which allied MWCNTs were first made through catalyst-assisted chemical vapor deposition (CVD) and later infiltrated through PU solution. The resulting MWCNT-PU composites presented a conductivity of 50–100 S/m and alterable resistance variation for strains up to 40%. Graphene, additional material in the carbon family, had been progressively applied for stretchable conductors by a smart combination with suitable elastomers (Kuilla et al., 2010; Xu and Zhu, 2012). According to Lee et al. (2012) for

example, a composite occupied of PU and functionalized graphene sheets could approach an elongation at a break of 374%, however retaining a conductivity of 1.2×10^{-5} S/cm.

Silver (Ag) nanostructures had also been intensively examined as a conductivity boosting factor for stretchable conductors. Zhu and Xu (2012) reported that their AgNWs (Ag nanowires) inserted PDMS composite attained a high conductivity of 5285 S/cm in a stretchable strain range of 0% to 50%. Lee et al. (2012) made networks of very lengthy AgNWs on Ecoflex utilizing a vacuum filtration and transfer technique, and they demonstrated high transparency of 90% to 96%, the sheet resistance of 9–70 Ω/sq, and good stretchability of >460%. Araki et al. (2011) formed Ag flakes PU composites through emulsion mixing and attained high stretchability up to 600% and low resistivity of 2.8×10^{-4} Ω¨ cm. In another interesting method, PU gold nanoparticle (AuNP) composites were prepared through vacuum-assisted flocculation or layer-by-layer assembly, and they presented an extreme conductivity of 11,000 S/cm and stretchability of 486% (Kim et al., 2013). Furthermore, AuNPs in these composites could be restructured under stress, permitting electronic regulation over mechanical properties (Sadhu and Bhowmick, 2004; Lang et al., 2009).

5.2.2. Stretchable Field-Effect Transistors and Memories

The common techniques of fabricating stretchable FETs (field-effect transistors) comprise the combined usage of stretchable conductors and rigid gate stack, implementation of wavy structures of the inorganic materials, and realization of composite FETs or organically made of entirely stretchable components. Shin et al. (2011) fabricated FET series of suspended SnO_2 NWs with wavy intersects and revealed high stretchability up to 40% and current on/off ratios of 10^6. Sekitani et al. (2008) fabricated a huge area stretchable active matrix comprising 19 × 37 organic transistors, integrating an SWCNT-founded elastomeric conductor. The device could be extended up to 70% both biaxially and uniaxially without mechanical fracture. Moreover, Kim *et al.* formed stretchable CMOS (complementary metal-oxide-semiconductor) inverters and 3 step ring oscillators on PDMS. Those devices implementing wavy structures of single-crystalline Si (silicon) nanoribbons presented stable oscillation frequency of ~3 MHz and high gains of 100, even under a 5% strain (Ghosh and Chakrabarti, 2000; Kojio et al., 2010).

Lately, Jeong's group developed stretchable transistors prepared completely of stretchable components (Shin et al., 2011). They utilized a poly SBS (styrene-*b*-butadiene-*b*-styrene) fiber mat as an elastomeric substrate. Polyelectrolyte gel, Au nanosheets, and P3HT (poly(3-hexylthiophene) nanofibers were employed for gate dielectric, electrodes, and active channel, correspondingly. The comprehensive device structures are presented in Figure 5.2(a)–(c). Au nanosheet electrodes were made through a transfer procedure utilizing P3HT fibers and PDMS pillars were electrospun on the substrate across drain electrodes and source. The transistors were reversibly extended up to a 70% strain ($\varepsilon = 0.7$), as revealed in Figure 5.2(d).

Not merely mechanically, however also electrically, the transistors showed reproducible performance up to 1500 cycles of stretching retrieval at ε = 0.7 (Figure 5.2(e) and (f)). The transistors displayed high hole mobility of 18 $cm^2/V^{¨}$ s and an on/off ratio of 10^5 even under ε = 0.7.

Likened to stretchable transistors, stretchable memories had been less examined. Flexible memories had been developed as a significant component of flexible electronics. For instance, Ouyang et al. (2004) prepared organic resistive memories from a polystyrene film comprising 8-hydroxyquinoline and AuNPs that were inserted amongst two metal electrodes. Ji et al. (2013) made a twistable memory cell series adopting a one diode-one resistor (1D-1R) structure and numerous organic materials for resistor components and diode. Though their memory cell range stably showed high on/off ratios of $>10^3$ up to a bendy angle of 30°, it was cracked at a strain of 2.03%. Lai et al. (2014) made a stretchable organic memory with a bent structure, where a blend of polymer compound and wrinkled graphene bottom electrode was utilized. After a blend of poly(3-butylthiophene (P3BT) and poly(methylmethacrylate (PMMA 3), which worked as the active information storing, was spin-coated on a CVD grownup graphene sheet, the film stack was transmitted on the pre-strained PDMS substrate. This caused a wrinkled organic memory structure, as revealed in Figure 5.3(a). This memory moved from 0 (a low-current state) to 1 (a high-current state) at a threshold voltage of 2.6 V, and the state was firmly maintained even after the exclusion of the applied voltage, which is a usual feature of non-volatile memory (Figure 5.3(b)). As shown in Figure 5.3(c) and (d), the memory behavior was not worsened through a strain up to 50% and the data retention reached 10^4 s (Bhattacharyya et al., 2008; Kim et al., 2011).

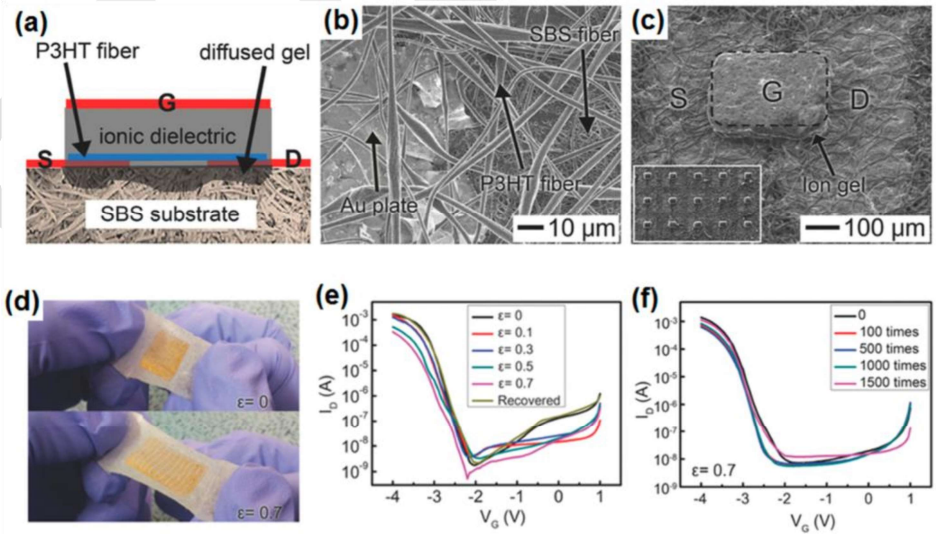

Figure 5.2. *(a) Schematic picture; (b) focused SEM image; and (c) low-magnification SEM image of a high stretchable transistor comprising completely of stretchable components; (d) photo images of the stretchable transistor range at two strain states (ε = 0 and 0.7); ID-VG curves relying on (e) the*

applied strain and (f) the number of stretching release cycles at ε = 0.7. In (a) and (c), D, G, and S represent drain, gate, and source correspondingly.

Source: https://onlinelibrary.wiley.com/doi/abs/10.1002/adma.201400009.

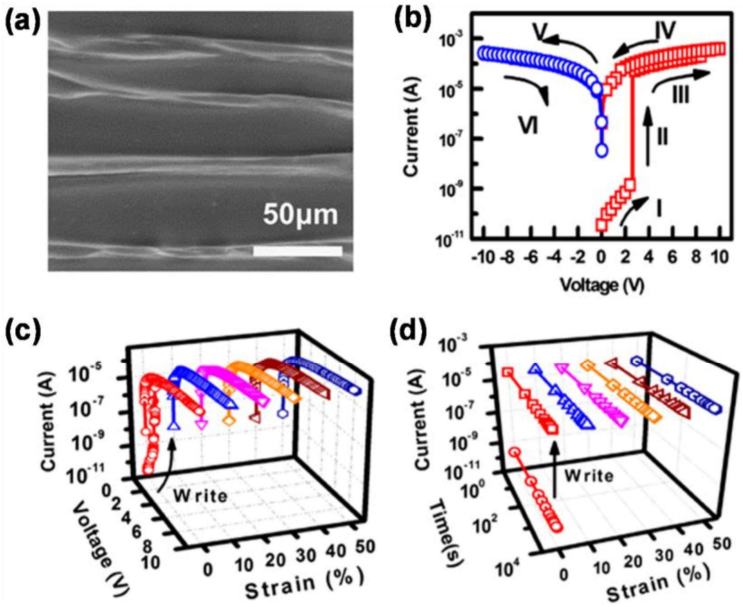

Figure 5.3. *(a) Top-view SEM image of the crumpled organic memory; (b) current-voltage characteristics displaying a memory behavior; strain dependent (c) memory switching; and (d) retention time.*

Source: https://www.nature.com/articles/am201385.

5.2.3. Stretchable Light-Emitting Diodes

The necessity for stretchable light-emitting systems is ever-growing in fields like rollable lamps, biocompatible light sources, and wearable displays. A common method of implementing stretchable shows is to combine elastic interconnects with organic LEDs or rigid inorganic (Park et al., 2009; Kim et al., 2011). Another method for stretchable displays is to implement intrinsically-stretchable OLEDs (organic LEDs), where all the components are stretchable. Filiatrault et al. (2012) fabricated LEECs (light-emitting electrochemical cells) utilizing stretchable Au/PDMS anodes and stretchable ruthenium (Ru)/PDMS emissive layers. However, they demonstrated huge area emission, the external quantum efficiency (EQE) and the strain tolerance of the devices were comparatively low. Pei's group produced transparent stretchable electrodes formed of fabricated (elastomeric polymer light-emitting device (EPLED) and AgNW-PUA (poly(urethane acrylate)composite, and through merging them with electroluminescent polymer layer (Liang et al., 2013, 2014). The EPLED could release light even at a high strain of 120%. The same group enhanced the performance of transparent stretchable electrodes by introducing graphene oxide (GO) to AgNW percolation networks, as displayed in Figure 5.4(a). The GO soldering turned out to decrease AgNW junction resistance and

overwhelm the inter-NW slip. The group fabricated PLED comprised of GO-AgNW-PUA composite electrodes, a polyethyleneimine (PEI) electron transporting layer, and a polymeric emissive layer (Figure 5.4(b)). The PLED could be extended up to 130% (Figure 5.4(c)) and undergo over 100 stretching cycles between 0% and 40% (Xiong et al., 2006; Bokobza, 2007).

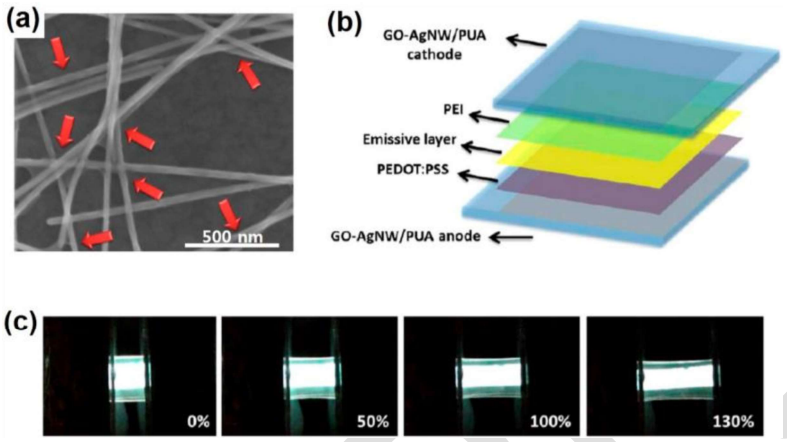

Figure 5.4. *(a) SEM image of GO (graphene oxide)-soldered AgNW (silver nanowire) junctions. Red arrows specify GO parts wrapping about AgNW junctions; (b) schematic drawing of a stretchable PLED structure; (c) optical photographs of a PLED (polymer light-emitting device) operating at 14 V under diverse strains.*

Abbreviations: PEI: polyethylenimine; PEDOT: poly(3,4-ethylene dioxythiophene); PSS: poly(styrene sulfonic acid); PUA: poly(urethane acrylate).

Source: https://pubs.acs.org/doi/10.1021/nn405887k.

5.2.4. Brief Summary

Representative accomplishments made in the stretchable electronics field are précised in Table 5.1. Of the three applications in this field, stretchable conductors had made the greatest development. They had attained tremendously large stretchability, up to 600%, however maintaining a high electrical conductivity of greater than 10^3 S/cm, which is the level needed for conventional interconnects and electrodes (Brosteaux et al., 2007; Park et al., 2014). However, easier techniques to fabricate such great performance stretchable conductors are required to be developed (Chen et al., 2007; Liu et al., 2015). Stretchable FETs had demonstrated good on/off ratios greater than 10^6; however, their stretchability still required to be further developed for the entirely stretchable applications. Stretchable memories are in their beginning. Stretchable LEDs had made a big development in terms of stretchability; however, their EQE is yet far inferior to their inorganic counterparts (Araby et al., 2014).

Table 5.1. Representative Accomplishments Made in the Field of Stretchable Electronics

Application	Material	Electrical Properties	Mechanical Properties
Stretchable conductors	PU-PPY composites	$\sigma = 10^{-5}$ S/cm	$\varepsilon_b = 160\%$
	Graphene sheets-PU composites	$\sigma = 1.2 \times 10^{-5}$ S/cm	$\varepsilon_b = 374\%$
	PU-PEDOT blends	$\sigma = 10–50$ S/cm	$\varepsilon = 200\%$
	3D PDMS-EGaIn	$\sigma = 24{,}100$ S/cm	$\varepsilon_b = 220\%$
	Ag flakes-PU composites	$\rho = 2.8 \times 10^{-4}$ Ω¨cm	$\varepsilon_b = 600\%$
Stretchable FETs and memories	SnO_2 NWs/wavy interconnects	On/Off ratio = 10^6	$\varepsilon_b = 40\%$
	P3HT/PS-PCBM/PEN	On/Off ratio > 10^3	$\varepsilon_b = 2.03\%$
	SBS fiber mat/P3HT nanofibers/polyelectrolyte gel	On/Off ratio = 10^5	$\varepsilon = 70\%$
	SWCNT-elastomer composites	On/Off ratio > 10^3	$\varepsilon_b = 70\%$
	PMMA-P3BT/PDMS	Data retention = 10^4 s	$\varepsilon_b = 50\%$
Stretchable LEDs	Ru-PDMS/Au-PDMS	EQE < 1%	$\varepsilon_b = 27\%$
	GO-AgNW-PUA composites/PEDOT:PSS/PEI	Current efficiency = 2.0 cd/A	$\varepsilon_b = 130\%$
	AuNW-PUA composites	EQE = 4%	$\varepsilon_b = 120\%$

Abbreviations: PU: Polyurethane; PCBM: ((6,6)-Phenyl-C_{61}-butyric acid methyl ester); PMMA: Poly(methylmethacrylate); PPY: Polypyrrole; PEN: Polyethylene naphthalate; SWCNT: Single-walled carbon nanotube; P3HT: Poly(3-hexylthiophene); P3BT: Poly(3-butylthiophene).

5.3. Stretchable Sensors

Though there are an extensive variety of sensors that had been developed to sense a huge number of materials or stimuli, they could be divided into two types: chemical sensors and physical sensors. Chemical sensors identify chemical species in the liquid phase or gas phase, whereas physical sensors notice physical stimuli like strain, temperature, and pressure. Despite this variation in sense targets, the two groups of sensors take benefit of the same sensing principles, which are founded on a variation in the physical properties of a device or sensing material, like capacitance, optical reflectance, and electrical resistance (Mahar et al., 2007). In the sensors field, the demand for stretchable sensors had been rising more and more for exceptional applications like implantable health monitors or body-conformable, electronic skins for intelligent robots and wearable sensory textiles (Thakur, 1988; Perez et al., 2009).

5.3.1. Stretchable Strain Sensors

Strain sensors are devices to exactly detect numerous mechanical deformations like compression, elongation, and bending. In the traditional field of structural health checking, comparatively low stretchability of below 1% would be sufficient for the application. Though for stretchable strain sensors that are the emphasis here, high stretchability is needed in addition to conventional sensor requirements like as good stability, fast response, and high sensitivity. Conventional metal founded strain sensors display the maximum strain of only around 5% and a gauge factor of ~2. Graphene sheets coated on the polymeric substrates had involved great interest, particularly in the aspect of sensitivity (Pandey et al., 2013). Although they had attained a colossal gauge factor of ~10^6, their stretchability was not up to mark (<10%). In comparison, CNT films on elastomeric substrates had shown large stretchability. For instance, Fan et al. (2012) fabricated strain sensors from the CNT networks covered on PU multifilaments and displayed a huge, reversible stretchability of 400%. Gauglitz (2005) fabricated vertically associated SWCNT films on the PDMS substrate and revealed high stretchability of 280% and low creep of 3% at a 100% strain. Regardless of the high stretchability, the measurement factor of the CNT elastomer composites was comparatively low (<5). As another method for recognizing stretchable strain sensors, certain research groups had utilized broken metal film structures on an elastomeric substrate. Puers (1993) formed buckle and microcracks structures in Ti (titanium) films crackled on PDMS through mechanical stretching, and Lacour et al. (2006) made tri-branched microcracks in the Au films electron beam evaporated on the PDMS. Though these strain sensors were simply fabricated and demonstrate strain-dependent resistance alteration, the repeatability of resistance signals required to be further guaranteed (Carone et al., 2002; Faseena et al., 2014).

AgNW-elastomer composites had also been keenly applied for stretchable strain sensors. Zhu and Xu (2012) formed a stretchable capacitive strain sensor by inserting AgNW films on both surfaces of a PDMS sheet. The capacitance of the sensor altered linearly and reproducibly with the functional strain in the range of 0% to 50%. Though, its gauge factor was only ~1. Kim et al. (2013) executed a stretchable resistive strain sensor, having the same approach. PDMS-AgNWs-PDMS sandwich-structured strain sensor (Figure 5.5(a)) presented reproducible resistance alterations under a range of linear strain of 0% to 70% and however under a bending strain (Figure 5.5(b) and (c)). This strain sensor presented nearly no hysteresis up to a strain of 40%, and hysteresis behaviors looked at a 60% strain with occupied resistance recovery at 0 strain. Human motion detection was also confirmed utilizing the strain sensor (Figure 5.5(d)).

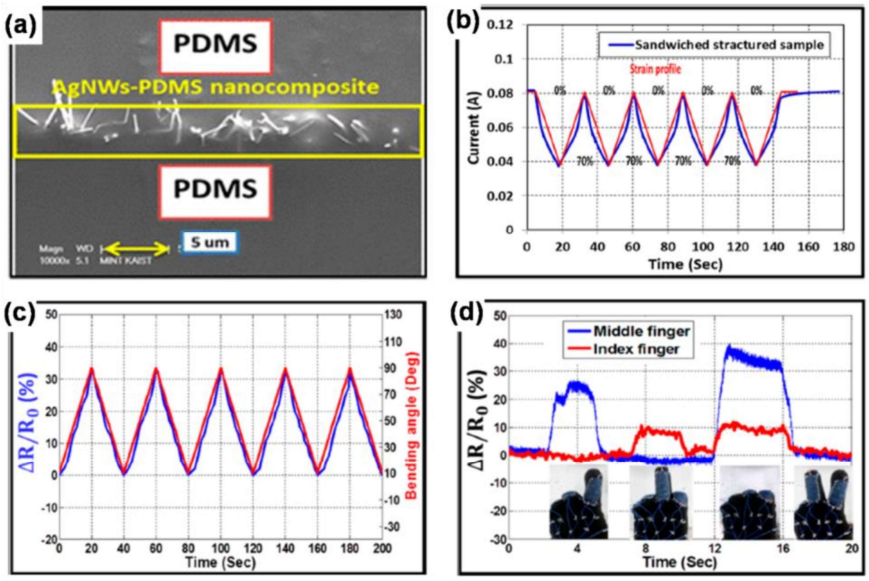

Figure 5.5. *(a) Cross-sectional SEM picture of PDMS-AgNWs-PDMS sandwich-structured strain sensor. Repeated replies of the strain sensor (b) to stretching releasing cycles at a strain of 70%; and (c) to bending cycles in the bending angles of 10°–90°; (d) presentation of finger motion detection utilizing the strain sensor.*

Source: https://pubs.acs.org/doi/10.1021/nn501204t.

5.3.2. Stretchable Pressure Sensors

Disparate strain sensors, which frequently detect lateral deformations, pressure sensors identify the magnitude of force vertically performing on a unit area of a plane. The main technique for the execution of stretchable pressure sensors is to mix a conductive matter with an elastomer in a precisely devised structure or a composite. In the methods utilizing composite materials, conductive nanostructures like metal nanowires/nanoparticles, CNTs, and CBs, are spread through an insulating elastomer and a resistive alteration under a pressure is measured. Though, the uniform distribution of conductive nanostructures is however to be confirmed more. As a marginally different approach, Liang et al. (2013) covered a PU foam with PPY by soaking the PU foam in a solution comprising naphthalene di-sulfonic acid and pyrrole monomer followed by *in situ* polymerization. They revealed real-time monitoring of the ribcage movement through breathing, utilizing this PPY-coated PU foam (Abbati et al., 2003; Vicentini et al., 2007).

More lately, numerous research groups had developed distinct device structures to attain highly-sensitive pressure sensors. Joo et al. invented a capacitive pressure sensor comprising of a PMMA dielectric layer and an AgNW-embedded PDMS electrode. Regardless of its high sensitivity (>3.8 kPa^{-1}), but, it was not stretchable. Park et al. invented a stretchable pressure sensor that comprised of Au-covered PDMS micropillars (top layer) and PANI nanofibers (bottom layer). This sensor functioned by measuring an alteration of contact resistance amongst the two layers under

applied pressure. They attained a high sensitivity of 2.0 kPa^{-1}, a less detection limit of 15 Pa, biaxial stretchability of 15%, a fast response time of 50 ms, from this sensor. As revealed in Figure 5.6(a), the PDMS micro-pyramids were covered with a PEDOT: PSS-PUD (PU dispersion) mixture, which operated as a piezoresistive electrode. Upon the application of pressure, every pyramid inclines to spread laterally, and this rises the contact perimeter (W_{PE}), contact interface area (A_{CI}), and the thickness of the existing path (D_{PE}), thus increasing the current conduction (Figure 5.6(b)). This sensor functioned well even at a high elongation of 40% and presented a very high sensitivity of 10.32 kPa^{-1} at that elongation (Figure 5.6(c)).

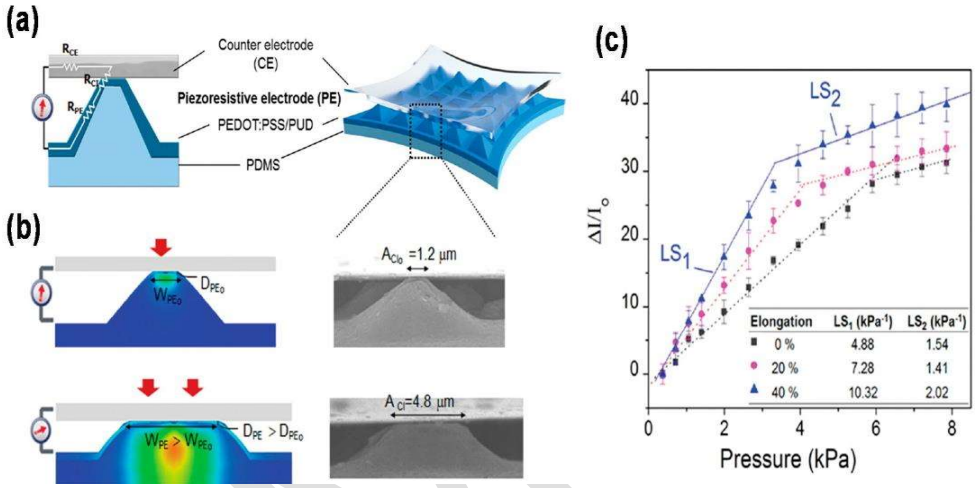

Figure 5.6. *(a) Schematic image of a micro-pyramid PDMS array. Discrete PDMS pyramids are covered with a PEDOT: PSS-PUD (Polyurethane dispersion) mixture, which assists as a piezoresistive electrode; (b) finite element analysis data displaying stress distributions and SEM pictures at diverse magnitudes of pressures; (c) relative existing changes relying on the applied pressure, however, the sensor is stretched to a specific elongation. Here, LS1 and LS2 signify the linear sensitivities in particular regions.*

Source: https://onlinelibrary.wiley.com/doi/abs/10.1002/adma.201305182.

5.3.3. Stretchable Temperature Sensors

Stretchable temperature sensors had attracted increasing attention, particularly for body-attachable applications. The traditional resistance temperature detector (RTD) takes benefit of the principle that a conductor's resistance alters with temperature. Though, good metals like platinum (Pt) and Au that are usually utilized for temperature sensors don't have stretchability by themselves. To overwhelmed this shortcoming, Chen et al. (2007) utilized a twisting structure of Au and joined it with porous PU. Their temperature sensor displayed good linearity of resistance alteration, good air-permeability, and good stretchability. Likewise, Liu et al. (2015) utilized a coiled structure of graphene that was fixed inside PDMS. This graphene elastomeric offered nonlinear resistance variation with the temperature

in the range of 3°C to 100°C and tolerance to strain up to 50%. Thakur (1988) activated a TFTV(thin-film transistor) array with a stretchable PANI nanofiber temperature sensing constituent. The PANI nanofiber sensors and SWCNT TFTs were first prepared on poly(ethylene terephthalate (PET) films, and then they were inserted onto Ecoflex. This temperature sensor showed a high resistance sensitivity of 1.0% per °C, mechanical stability to biaxial strain up to 30%, and a response time of 1.8 s. Moreover, Vicentini et al. (2007) invented an entirely elastomeric gated temperature sensor. For that, a PEDOT: PSS-PUD composite was utilized as a drain, source, and gate material, PU as a gate dielectric, and decrease graphene oxide (R-GO)-PU complex as a temperature sensing channel layer (Figure 5.7(a)). This temperature sensor could expand up to a strain of 70% and showed a high sensitivity of 1.34% and steady response to temperature, however, after 10,000 cycles of stretching at a 30% strain (Figure 5.7(b)).

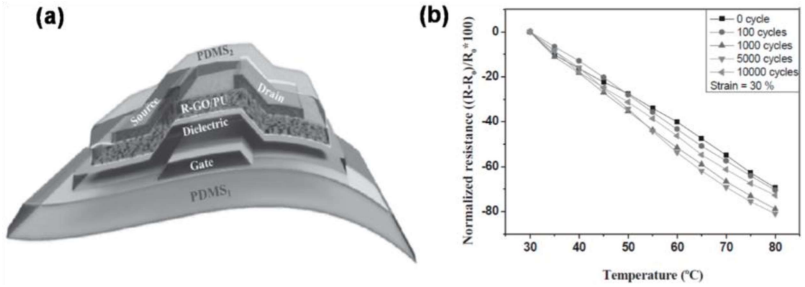

Figure 5.7. *(a) Schematic drawing of a whole elastomeric gated temperature sensor; (b) reply of the temperature sensor after cyclic stretching of 0–10,000 cycles at a strain of 30%. Source: https://onlinelibrary.wiley.com/doi/10.1002/adma.201504441.*

5.3.4. Brief Summary

Representative successes made in the field of stretchable sensors are précised in Table 5.2 (Yoshikawa et al., 2006).

Table 5.2. Representative Successes Made in the Field of Stretchable Sensors

Application	Material	Sensing Properties	Mechanical Properties
Stretchable strain sensors	Graphene woven fabric/PDMS	Gauge factor = ~10^6	ε_b = 10%
	CNT networks/PU multifilament	Gauge factor = ~5	ε_b = 400%
	PDMS/AgNWs/PDMS	Gauge factor = ~5	ε = 0%–70%
	AgNWs/PDMS	Gauge factor = ~1	ε = 0%–50%
Stretchable pressure sensors	PPY-coated PU foam	Sensitivity = 0.0007 mS/N	ε > 1,000%
	AgNW-embedded	Sensitivity > 3.8	Not stretchable

	PDMS/PMMA	kPa^{-1}	
	Micro-pyramid PDMS/PEDOT: PSS-PUD blend	Sensitivity = 10.32 kPa^{-1} Detection limit = 23 Pa	$\varepsilon > 40\%$
	Au-coated PDMS micropillars/PANI nanofibers	Sensitivity = 2.0 kPa^{-1} Detection limit = 15 Pa	ε_b (biaxial) = 15%
Stretchable temperature sensors	SWCNT TFT-PANI nanofiber/PET/Ecoflex	Sensitivity = 1.0% per °C	ε_b (biaxial) = 30%
	Graphene embedded in PDMS	Nonlinear *R versus T* in 30–100°C	ε_b = 50%
	PDMS/PEDOT: PSS-PUD composite/PU/(R-GO)-PU composite	Sensitivity = 1.34% per °C	ε_b = 70%

Abbreviations: PANI: Polyaniline; PET: Poly(ethylene terephthalate); TFT: Thin-film transistor.

Altogether three applications had made incredible achievements. Specifically, stretchable strain sensors had displayed great performance in both gauge factor and mechanical stretchability and described their functionality in the area of motion finding. Simple mixtures of elastomers and conductive nanostructures had been confirmed to work efficiently for this application. Stretchable pressure sensors seem to required further development in stretchability, though their sensitivity is sufficiently good. Certain stretchable temperature sensors had fulfilled both requirements of temperature sensitivity and stretchability. Though their material combinations and structures are in general complicated, and further exertions to develop simpler structures would be essential.

5.4. Stretchable Energy Harvesters

As the global warming problem caused due to the usage of fossil fuel had surged, new energy generation approaches had been in excessive demand. Numerous techniques of harvesting energy from various sources were developed to decrease the consumption of fossil fuel, and few of them had already come into our daily life. Photovoltaic (or solar) cells that transform solar energy into electrical energy are a typical instance. Thermoelectric energy harvesting and piezoelectric energy harvesting had also been enhancing their application areas. Usually, these energy harvesters were formed of inorganic materials like PZT(lead zirconate titanate), Bi_2Te_3 (bismuth telluride), and Si all of which are brittle. Due to the sharply increasing usage of wearable or portable low-power-operated electronics, the necessity for stretchable energy harvesters had been rising larger.

5.4.1. Stretchable Solar Cells

Organic photovoltaic (OPV) cells had been of enhancing interest in numerous applications, mainly for electronic skin, intelligent robotics, and wearable electronics. Around a decade after discovery of record-high power conversion efficiency (PCE) of 2.5% for OPV cells, Mitsubishi Chemical substituted the record with 9.2%. For the conventional bulk heterojunction OPV cells, indium tin oxide (ITO) is utilized as a transparent electrode and it is covered with an hole transport layer (HTL), usually made of PEDOT: PSS. Over the HTL, an active layer that is a blend of acceptor and donor materials is covered by the solution casting method or co-deposition. Till now, the most efficient OPV cells, the PCE of which is above 3.5%, had come from solution-cast P3HT: PCBM ((6,6)-phenyl-C_{61}-butyric acid methyl ester) mixtures. This device structure and material combinations had been maintained as a basic platform for the understanding of stretchable solar cells. A straightforward method of executing a stretchable solar cell is to connect highly effective, however rigid inorganic cells with the stretchable interconnects. Lee et al. (2009) first fabricated GaAs (gallium arsenide) microcells on Si substrate and moved them to the PDMS substrate. Afterward, arc-shaped Au interconnects were transform to bridge the microcells. This microcell array presented a PCE of 13%, a high fill factor of 0.79; however, its stretchability was restricted to below 30%.

Hsu et al. (2011) made stretchable organic solar cells founded on organic materials explained above. They spin-coated P3HT: PCBM layer and PEDOT: PSS layer and placed liquid metal consecutively on pre-strained PDMS substrate. Then, buckles were convinced to the layer stack upon relaxing the PDMS substrate. This buckle structured solar cell displayed endurance to strain up to 22.2%. However, its fill factor (0.38) and PCE (1.2%) were not good. Utilizing a similar material combination for the active layer, an ultrathin OPV cell was invented (Khan et al., 2010). As shown in Figure 5.8(a), the entire thickness of the solar cell is merely 1.9 μm. When this OPV cell fixed on a PET film was attached to a pre-stretched elastomer, it might tolerate a huge compression of up to 80% (Figure 5.8(b)). This solar cell showed enhanced performance with a PCE of 4.2% and a fill factor of 0.61. Though almost reinstated to the actual value after re-stretching it to its early state, the short circuit current of the solar cell reduced with growing compression from 0% to 80% (Figure 5.8(c)).

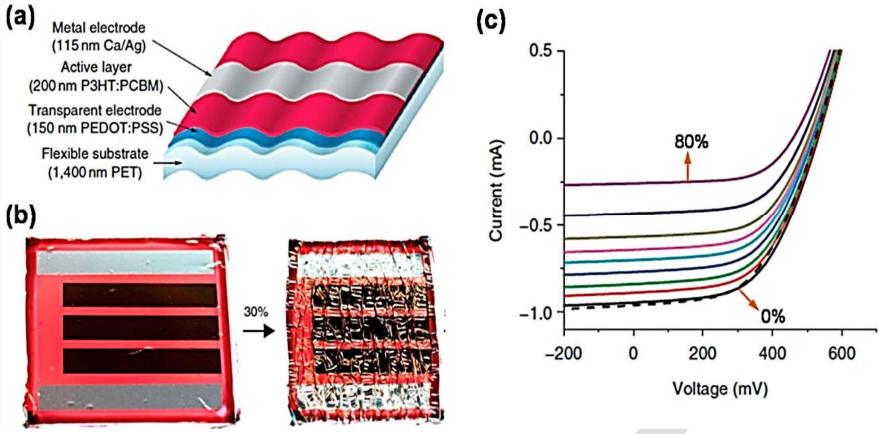

Figure 5.8. *(a) Diagram of the ultrathin organic solar cell; (b) stretchable solar cell made simply through attaching the ultrathin cell to a pre-stretched elastomer. It could be re-stretched and compressed; (c) current-voltage curves of the solar cell relying on the compression in the range of 0%–80%. Between the black (0%) and purple (80%) lines, individual colors signify the compression growing with a step of 10%. The black dashed line signifies the device after being restored to its early state.*

Source: https://www.nature.com/articles/ncomms1772.

5.4.2. Other Stretchable Energy Harvesters

Piezoelectric energy harvesters transform diverse mechanical stimuli into electricity. Flexible piezoelectric energy harvesters had been stated, which employed numerous nanostructured materials like ZnO nanorods/nanowires, PZT nanowires/ribbons, and polyvinylidene fluoride (PVDF) nanofibers on flexible substrates like paper and polyimide. For instance, El-Tantawy et al. (2009) had got a high-power density of 2.4 μW¨ cm^{-3} utilizing a PZT NW-PDMS nanocomposite. Though these energy harvesters were confirmed to be highly flexible, they needed stretchability. Lee et al. (2009) made a stretchable hybrid nanogenerator (NG) that integrated graphene as the top electrode, poly(vinylidene fluoride-*co*-trifluoro ethylene) as the energy-harvesting layer, and PDMS-CNT compound as the bottom electrode. Their NG might stretch up to a strain of 30%; however, its output power was not huge enough, probably because of the insufficient pyroelectricity and piezoelectricity of the harvesting material. Chen et al. (2013) showed a hyper SEG (stretchable elastic generator) by forming stretchable very long nanowire percolation (VLNP) electrodes on a piezoelectric elastic composite (PEC) comprised of lead magnesium niobate-lead titanate (PMN-PT) particles and MWCNTs discrete in silicone rubber (SR) (Figure 5.9(a)). This SEG displayed a huge, reversible stretchability of ~200% (Figure 5.9(b)) and high-power output of ~4 V and ~500 nA (Figure 5.9(c)).

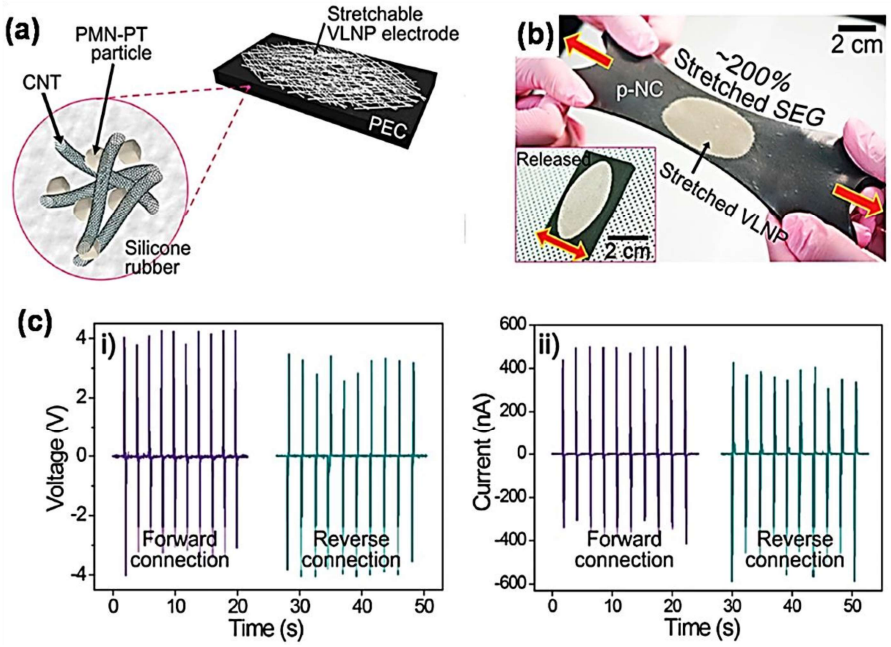

Figure 5.9. *(a) Diagram picture of the hyper-stretchable nanocomposite generator (SEG); (b) the SEG could be stretched and free without harm; (c) generated (i) open-circuit voltage and (ii) short-circuit current relying on periodic stretching releasing cycles at a strain of 200%. Source: https://onlinelibrary.wiley.com/doi/full/10.1002/adma.201500367.*

Thermoelectric energy harvesting is a method to produce electrical power from discarded heat. In latest years, organic thermoelectric generators (TEGs) had gained much attention because of numerous advantages over their inorganic counterparts, like as good processibility, flexibility low cost, and low thermal conductivity. The key materials for the organic TEGs were conducting polymers and composites founded on them. Regardless of many successes in flexible organic TEGs, research on stretchable TEGs had been rare. Kim et al. (2008) made a wearable TEG comprising of inorganic thermoelectric components made on glass fabric. Though this TEG fixed in PDMS was flexible, thin, and showed a high output power density of 28 mW¨ g^{-1} at a ΔT = 50 K, it was not stretchable. Liang et al. (2013) took the initial step toward a stretchable TEG. They made PPY-SWCNT nanocomposites utilizing an *in situ* oxidative polymerization technique, as depicted in Figure 5.10(a). As a result of the reaction, SWCNTs covered with PPY were got, and their films were prepared through vacuum filtration technique. This nanocomposite film displayed greatly enhanced thermoelectric performance with a power factor of 19.7 µW¨ m^{-1}¨ K^{-2}, which is the biggest value for PPY composites. Additionally, it could be stretched through 2.6% (Figure 5.10(b)); however, its stretchability still required to be enhanced.

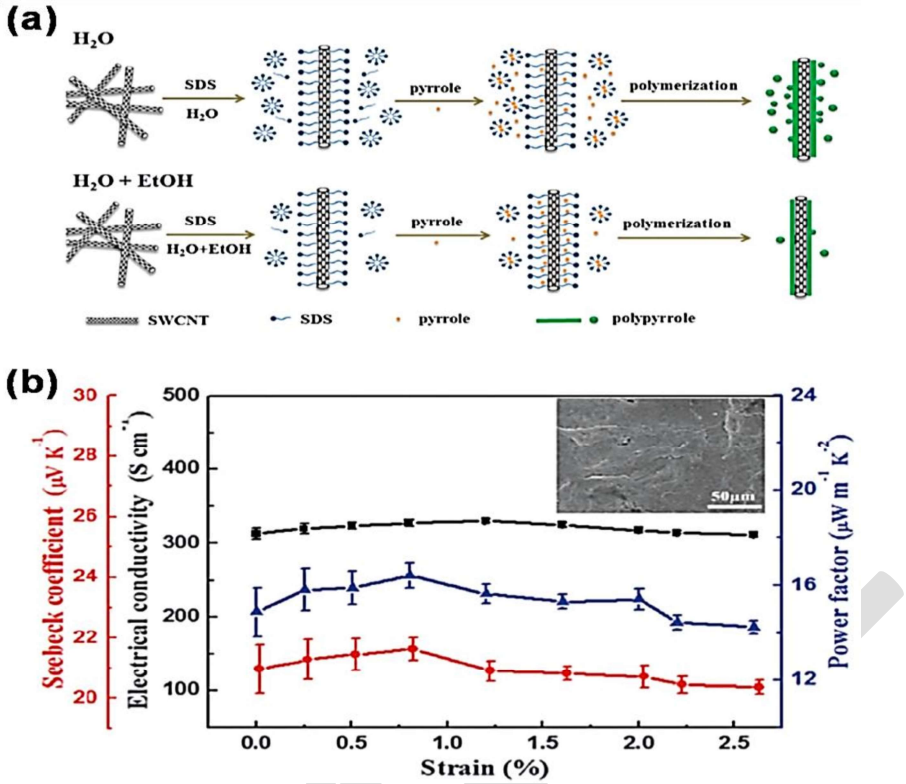

Figure 5.10. *(a) Schematic image for the preparation processes of PPY-SWCNT nanocomposites; (b) reliance on the thermoelectric performance of the composite on the mechanical stretching. The inset is an SEM picture of the composite film after a 2.5% stretching.*

Source: https://pubs.rsc.org/en/content/articlelanding/2016/TC/c5tc03768a#!divAbstract.

5.5. Summary

Managing with novel technology waves, like intelligent robotics, stretchable/wearable devices, and body-conformable devices, the demand for the conductive elastomers had been whirled. As a reply to this demand, a diversity of research had been intensively started to progress optimal conductive elastomers. Though similar structures and the similar material combination had been employed sometimes in diverse fields of application, comprehensive strategies changed depending on the goal and the target application. In this chapter, research exertions put into three fields of stretchable technology, which are stretchable sensors, stretchable energy harvesters, and stretchable electronics, are reviewed. In every field, how conductive elastomers were integrated into representative devices, exactly how those materials were made, and what performance had been attained with the conductive elastomers are introduced and analyzed. In numerous cases, insulating elastomers like PU, PDMS, and SR were combined either with the conducting polymers like PANI, PPY, and PEDOT: PSS, or with conductive nanostructures like as CNTs AgNWs, and graphene for the execution of conductive elastomers. Further, the conductive elastomers, stretchable functional materials were also integrated to award the main functions of designed devices. Ru/PDMS emissive layer for a stretchable display,

PMN-PT particles spread in PDMS for a stretchable piezoelectric energy harvester, and P3HT nanofibers for a stretchable FET, are those instances. PDMS had been most extensively employed as an elastomeric substrate for most applications. As pronounced attainments, a stretchable conductor had shown stretchability of up to 600% and high conductivity of more than 10^3 S/cm. Similarly, a stretchable strain sensor had confirmed stretchability of 400% with a gauge factor of ~5. Though, issues like the development of easy fabrication methods and reliability of conductive elastomers are still to be resolved. Regardless of the notable successes in stretchable applications encouraged by conductive elastomers, it is also factual that numerous stretchable technologies still required to be further explored.

References

Abbati, G., Carone, E., D'Ilario, L., & Martinelli, A., (2003). Polyurethane-polyaniline conducting graft copolymer with improved mechanical properties. *J. Appl. Polym. Sci., 89*, 2516–2521.

Ahn, J. H., & Je, J. H., (2012). Stretchable electronics: Materials, architectures and integrations. *J. Phys. D Appl. Phys., 45*, 103001.

Araby, S., Meng, Q., Zhang, L., Kang, H., Majewski, P., Tang, Y., & Ma, J., (2014). Electrically and thermally conductive elastomer/graphene nanocomposites by solution mixing. *Polymer, 55*, 201–210.

Araki, T., Nogi, M., Suganuma, K., Kogure, M., & Kirihara, O., (2011). Printable and stretchable conductive wirings comprising silver flakes and elastomers. *IEEE Electron Device Lett., 32*, 1424–1426.

Balint, R., Cassidy, N. J., & Cartmell, S. H., (2014). Conductive polymers: Towards a smart biomaterial for tissue engineering. *Acta Biomater., 10*, 2341–2353.

Benight, S. J., Wang, C., Tok, J. B. H., & Bao, Z., (2013). Stretchable and self-healing polymers and devices for electronic skin. *Prog. Polym. Sci., 38*, 1961–1977.

Bhadra, S., Khastgir, D., Singha, N. K., & Lee, J. H., (2009). Progress in preparation, processing and applications of polyaniline. *Prog. Polym. Sci., 34*, 783–810.

Bhattacharyya, S., Sinturel, C., Bahloul, O., Saboungi, M. L., Thomas, S., & Salvetat, J. P., (2008). Improving reinforcement of natural rubber by networking of activated carbon nanotubes. *Carbon, 46*, 1037–1045.

Bokobza, L., (2007). Multiwall carbon nanotube elastomeric composites: A review. *Polymer, 48*, 4907–4920.

Bokobza, L., Garnaud, G., & Mark, J. E., (2002). Effects of filler particle/elastomer distribution and interaction on composite mechanical properties. *Chem. Mater., 14*, 162–167.

Brosteaux, D., Axisa, F., Gonzalez, M., & Vanfleteren, J., (2007). Design and fabrication of elastic interconnections for stretchable electronic circuits. *IEEE Electron Device Lett., 28*, 552–554.